High-level expression of STING restricts susceptibility to HBV by mediating type III IFN induction

Running title: STING-mediated restriction of HBV

Hiromichi Dansako[*,1], Hirotaka Imai[1], Youki Ueda[1], Shinya Satoh[1], Kunitada Shimotohno[2], Nobuyuki Kato[1]

[1]Department of Tumor Virology, Okayama University Graduate School of Medicine, Dentistry and Pharmaceutical Sciences, Okayama, Japan

[2]Research Center for Hepatitis and Immunology, National Center for Global Health and Medicine, Chiba, Japan.

[*]Corresponding author. Tel: +81 86 235 7386; E-mail: dansako@md.okayama-u.ac.jp

Keywords: hepatitis B virus, hepatocellular carcinoma, host innate immune response, STING, type III interferon

Abstract

Hepatitis B virus (HBV) is a hepatotropic DNA virus causing hepatic diseases such as chronic hepatitis, liver cirrhosis, and hepatocellular carcinoma. To study HBV, human hepatoma HepG2 cells are currently used as an HBV infectious cell culture model worldwide. HepG2 cells exhibit susceptibility to HBV by exogenously expressing sodium taurocholate cotransporting polypeptide (NTCP). We herein demonstrated that human immortalized hepatocyte NKNT-3 cells exhibited susceptibility to HBV by exogenously expressing NTCP (NKNT-3/NTCP cells). By comparing the cGAS-STING signaling pathway in several NKNT-3/NTCP cell-derived cell clones, we found that STING was highly expressed in cell clones exhibiting resistance but not susceptibility to HBV. High-level expression of STING was implicated in HBV-triggered induction of type III IFN and a pro-inflammatory cytokine, IL-6. In contrast, RNAi-mediated knockdown of STING inhibited type III IFN induction and restored the levels of HBV total transcript in an HBV-infected cell clone exhibiting resistance to HBV. These results suggest that STING regulates susceptibility to HBV by its expression levels.

STING may thus be a novel target for anti-HBV strategies.

Introduction

Hepatitis B virus (HBV) is a hepatotropic virus classified into the *Hepadnaviridae* family. HBV infection causes chronic hepatitis, liver cirrhosis, and finally hepatocellular carcinoma (HCC) [1, 2]. The progression of hepatic diseases is tightly associated with the HBV-triggered host innate immune response and inflammatory response. To prevent the progression of hepatic diseases, it is important to suppress the HBV-triggered host innate immune response and inflammatory response.

The cytoplasmic DNA sensor, cyclic GMP-AMP synthetase (cGAS), is known to recognize viral DNA and other non-self exogenous DNAs as pathogen-associated molecular patterns (PAMPs) [3, 4]. After the recognition of non-self exogenous DNA, cGAS produces cyclic GMP-AMP (cGAMP) and then uses cGAMP to activate a stimulator of interferon genes (STING). STING mediates activation of the transcription factor interferon regulatory factor 3 (IRF-3) and subsequently the induction of interferon (IFN)-β (type I IFN) [5], IFN-λ1, λ2, and λ3 (type III IFN) [6]. Both type I and type III

IFNs stimulate the induction of numerous IFN-stimulated genes (ISGs) such as ISG15 and ISG56 through the JAK-STAT signaling pathway [7]. On the other hand, STING also mediates the induction of pro-inflammatory cytokines such as IL-6 and IL-8 through the NF-κB signaling pathway [8, 9]. As described here, both cGAS and STING are required for the innate immune response and inflammatory response. We previously reported that cGAS recognized HBV DNA and subsequently triggered an innate immune response in human hepatoma Li23 cells [10]. However, in that study, we could not examine the HBV-triggered inflammatory response, since Li23 cells were a human hepatoma cell line. To study HBV-triggered inflammatory responses, it will be necessary to establish an HBV infectious cell culture model from normal human hepatic cells rather than human hepatoma cells.

Sodium taurocholate cotransporting polypeptide (NTCP) is a functional receptor for HBV [11]. Human hepatoma HepG2 cells exhibit susceptibility to HBV by exogenously expressing NTCP [11]. HepG2/NTCP cells (HepG2 cells stably expressing exogenous NTCP) are currently used as an HBV infectious cell culture model for the study of HBV worldwide. However, we previously reported that HepG2 cells exhibited defective

expression of endogenous cGAS [10]. This result suggests that HepG2/NTCP cells cannot be used for the study of endogenous cGAS-triggered innate immune response and inflammatory response. Our previous study also showed that cGAS was expressed in immortalized human hepatocyte NKNT-3 cells [10]. In the present study, we established NKNT-3 cells exhibiting susceptibility to HBV by the exogenous expression of NTCP. In addition, we obtained several NKNT-3/NTCP-derived cell clones exhibiting susceptibility or resistance to HBV. Interestingly, STING was highly expressed in a cell clone exhibiting resistance to HBV. Here, we show that STING is an important host factor that regulates susceptibility to HBV by its expression levels. We also show that NKNT-3/NTCP cells are a novel HBV infectious cell culture model for the study of HBV-triggered innate immune responses and inflammatory responses.

Results

The immortalized human hepatocyte NKNT-3 cells exhibited susceptibility to HBV via their expression of exogenous NTCP.

Since HepG2 cells were a human hepatoma cell line and exhibited defective

81 expression of endogenous cGAS [10], we tried to establish HBV infectious cell culture
82 model from immortalized human hepatocyte NKNT-3 cells, which has been exhibited a
83 non-neoplastic phenotype [12] and the endogenous expression of cGAS [10]. HepG2
84 cells have been reported to exhibit susceptibility to HBV through their expression of
85 exogenous NTCP [11]. Therefore, to establish NKNT-3 cells exhibiting susceptibility to
86 HBV, we first prepared NKNT-3 cells stably expressing exogenous NTCP-myc
87 (designated NKNT-3/NTCP cells; Fig. 1A). The cell surface expression of NTCP was
88 detected in both NKNT-3/NTCP cells and HepG2/NTCP cells (HepG2 cells stably
89 expressing exogenous NTCP-myc), but not in NKNT-3/Control cells (NKNT-3 cells
90 stably expressing the control vector) (Fig. 1B). By using two kinds of inoculum,
91 HBV/NLuc (genotype C) [13] and HBV (the supernatant of HBV-replicating
92 HepG2.2.15 cells, genotype D) [14], we compared the levels of susceptibility to HBV in
93 NKNT-3/NTCP cells with that in NKNT-3/Control cells. After the infection with
94 HBV/NLuc or HBV, both level of NLuc activity and HBV total transcript were
95 increased in NKNT-3/NTCP cells in a time-dependent manner, but not in
96 NKNT-3/Control cells (Figs. 1C and 1D). We next compared the level of susceptibility

97 to HBV in NKNT-3/NTCP cells with that in HepG2/NTCP cells. The levels of NLuc
98 activity, HBV total transcript, and pgRNA in HBV/NLuc- or HBV-infected
99 NKNT-3/NTCP cells were almost ten times lower than those in HBV/NLuc- or
100 HBV-infected HepG2/NTCP cells (Figs. 1E and 1F). We further examined whether or
101 not the exogenous NTCP was functional in NKNT-3/NTCP cells. Cyclosporin A (CsA)
102 was previously reported to inhibit HBV entry by targeting NTCP [15]. When
103 administered before and during HBV inoculation, CsA inhibited the levels of HBV total
104 transcript in HBV-infected NKNT-3/NTCP cells as well as in HBV-infected
105 HepG2/NTCP cells (Fig. 1G). These results suggest that NKNT-3 cells exhibit
106 susceptibility to HBV by exogenously expressing functional NTCP.
107
108 **The level of susceptibility to HBV in NKNT-3/NTCP #28.3.8 cells approximated**
109 **that in HepG2/NTCP cells.**
110 Since susceptibility to HBV in NKNT-3/NTCP cells was lower than that in
111 HepG2/NTCP cells (Figs. 1E and 1F), we next tried to select a subcloned cell line
112 exhibiting higher susceptibility to HBV than NKNT-3/NTCP cells (Fig. 2A). During

three-round serial limited dilution, we obtained three distinct cell clones (#28, #28.3, and #28.3.8 cells, respectively; Fig. 2A) that met this criterion (Fig. 2B). Exogenous NTCP was expressed on the cell surface in all three clones (Fig. 2C). Among them, the NKNT-3/NTCP #28.3.8 cells exhibited the highest levels of HBV total transcript after HBV infection (Fig. 2D). Therefore, we next compared the levels of susceptibility to HBV in NKNT-3/NTCP #28.3.8 cells with those in HepG2/NTCP cells. Upon the infection with HBV/NLuc or HBV, both levels of NLuc activity (Fig. 2E) and HBV total transcript (Fig. 2F) in NKNT-3/NTCP #28.3.8 cells approximated those in HepG2/NTCP cells. Consistent with these results, Northern blot analysis also showed that the levels of HBV pregenomic RNA (pgRNA) and 2.1/2.3 kb RNA in NKNT-3/NTCP #28.3.8 cells were roughly the same as those in HepG2/NTCP cells after HBV infection (Fig. 2G). These results suggest that NKNT-3/NTCP #28.3.8 cells are useful as an HBV infectious cell culture model in the manner of HepG2/NTCP cells.

HBV triggered the induction of type III IFNs in NKNT-3/NTCP #28.3.25.13 cells exhibiting resistance to HBV.

During the three-round limited dilution, we obtained NKNT-3/NTCP #28.3.8 cells that exhibited higher susceptibility to HBV than the parent NKNT-3/NTCP cells (Figs. 2B and 2D). On the other hand, during the additional limited dilution (Fig. 3A), we unexpectedly obtained a cell clone (#28.3.25.13) exhibiting greater resistance to HBV compared with NKNT-3/NTCP #28.3.8 cells (Fig. 3B). We conjectured that the innate immune response might be induced in cell clones exhibiting resistance to HBV. To examine this possibility, we first compared the HBV-triggered innate immune responses among cell clones exhibiting susceptibility or resistance to HBV. At 5 days after HBV infection, ISG56 was strongly induced in NKNT-3/NTCP #28.3.25.13 cells, but not in NKNT-3/NTCP #28.3.8 cells (Fig. 3C). Since HBV-triggered ISG56 induction in NKNT-3/NTCP #28.3.25.13 cells was higher than that in #28.3. 30.20.3 cells (another cell clone exhibiting resistance to HBV, Fig. 3B), we mainly focused the innate immune response to HBV in NKNT-3/NTCP #28.3.25.13 cells. We first compared the time course of *ISG56* mRNA induction after HBV infection between NKNT-3/NTCP #28.3.8 and #28.3.25.13 cells (Fig. 3D). At 5 or 9 days after HBV infection, *ISG56* mRNA was strongly induced in NKNT-3/NTCP #28.3.25.13 cells, but not in #28.3.8 cells (Fig. 3D).

These results suggest that HBV infection induces the innate immune response in cell clone exhibiting resistance but not susceptibility to HBV. We next examined whether type I and/or type III IFN was required for *ISG56* mRNA induction after HBV infection in NKNT-3/NTCP #28.3.25.13 cells. Interestingly, at 9 days after HBV infection, *IFN-λ1* and *IFN-λ2/3* (type III IFN) mRNA, but not *IFN-β* (type I IFN) mRNA, were induced in NKNT-3/NTCP #28.3.25.13 cells (Figs. 3E and 3F). In addition, *IFN-λ1* mRNA (Fig. 3G), ISG15 (Fig. 3H), and ISG56 (Fig. 3H) were induced at 9 days after HBV infection, but not mock or ultraviolet-inactivated HBV (UV-HBV) infection, in NKNT-3/NTCP #28.3.25.13 cells. Consistent with these results, HBV induced *IFN-λ1* and *IFN-λ2/3*, but not *IFN-β* mRNA, in HBV-replicating HepG2.2.15 cGAS/STING cells stably expressing both exogenous cGAS and STING [10] (Fig. 3I). In addition, the induction levels of *IFN-λ1* and *IFN-λ2/3* mRNA in HepG2.2.15 cGAS/STING cells were higher than those in HepG2.2.15 cGAS GSAA/STING cells stably expressing both exogenous cGAS GSAA (the inactive mutant of cGAS) and STING [10]. These results suggest that HBV induces type III IFN through the cGAS/STING signaling pathway in NKNT-3/NTCP #28.3.25.13 cells, but not in #28.3.8 cells. These results also

suggest that the expression levels of cGAS/STING signaling pathway-associated host factor(s) are different between NKNT-3/NTCP #28.3.8 cells and #28.3.25.13 cells.

High-level expression of STING was implicated in HBV-triggered type III IFN induction in NKNT-3/NTCP #28.3.25.13 cells exhibiting resistance to HBV.

Since our results suggested that the expression levels of cGAS/STING signaling pathway-associated host factor(s) were different between NKNT-3/NTCP #28.3.8 cells and #28.3.25.13 cells, we next compared the levels of p-dGdC (the synthetic ligand for the cGAS/STING signaling pathway)-triggered type III IFN induction. We found that the p-dGdC-triggered *ISG56* and *IFN-lambda1* mRNA induction in NKNT-3/NTCP #28.3.25.13 cells was several times higher than that in NKNT-3/NTCP #28.3.8 cells (Fig. 4A). We next tried to identify the host factor(s) responsible for the higher responsiveness to p-dGdC in NKNT-3/NTCP #28.3.25.13 cells. Among cGAS/STING signaling pathway-associated host factor(s), we found that *STING* mRNA (Fig. 4B) and STING protein (Fig. 4C) were highly expressed in NKNT-3/NTCP #28.3.25.13 cells. These results suggest that the high-level expression of STING enhances

177 p-dGdC-triggered type III IFN induction in NKNT-3/NTCP #28.3.25.13 cells compared
178 with #28.3.8 cells. We further compared the phosphorylation levels of STING among
179 several NKNT-3/NTCP cell-derived cell clones. STING was highly phosphorylated in
180 p-dGdC-transfected NKNT-3/NTCP #28.3.25.13 cells, but not in #28.3.8 cells (Fig. 4D,
181 lower-left panel). In addition, STING was also highly phosphorylated in p–
182 dGdC-treated NKNT-3/NTCP #28.3.25 cells (the parent cells of #28.3.25.13) but not in
183 the parent cells, or in #28 and #28.3 cells (the common parent cells of #28.3.8, #28.3.25
184 and #28.3.25.13, respectively). *IFN-λ1* mRNA was strongly induced in NKNT-3/NTCP
185 cells highly phosphorylating STING such as NKNT-3/NTCP #28.3.25 and #28.3.25.13
186 cells (Fig. 4D, upper-left panel). Consistent with these results, the knockdown of
187 STING reduced *IFN-λ1* mRNA induction in p-dGdC-transfected NKNT-3/NTCP
188 #28.3.25.13 cells (Fig. 4D, upper-right panel). These results suggest that STING
189 regulate p-dGdC-triggered type III IFN induction by its expression level in
190 NKNT-3/NTCP cells.

191 We next examined whether high-level expression of STING was required for
192 HBV-triggered type III IFN induction in NKNT-3/NTCP #28.3.25.13 cells. We found

193 that knockdown of STING decreased the induction of *IFN-λ1* mRNA (Fig. 4E, upper
194 panel) and subsequently ISG56 (Fig. 4E, lower panel) in HBV-infected NKNT-3/NTCP
195 #28.3.25.13 cells. The knockdown of STING also increased the amounts of HBV total
196 transcript in HBV-infected NKNT-3/NTCP #28.3.25.13 cells (Fig. 4F). On the other
197 hand, the stable expression of exogenous STING, but not STING I200N which causes
198 the conformational disruption [16], increased the induction of *IFN-λ1* mRNA (Fig. 4G,
199 upper panel) and subsequently ISG56 (Fig. 4G, lower panel) in HBV-infected
200 NKNT-3/NTCP #28.3.8 cells. The stable expression of exogenous STING also
201 decreased the amounts of HBV total transcript in HBV-infected NKNT-3/NTCP #28.3.8
202 cells (Fig. 4H). These results suggest that high-level expression of STING is implicated
203 in HBV-triggered type III IFN induction in NKNT-3/NTCP #28.3.25.13 cells.
204
205 **High-level expression of STING was required for the HBV-triggered inflammatory**
206 **response in NKNT-3/NTCP #28.3.25.13 cells.**
207 Since high-level expression of STING mediated HBV-triggered type III IFN
208 induction in NKNT-3/NTCP #28.3.25.13 cells (Figs. 4D and 4E), we next examined

209 whether high-level expression of STING was implicated in the induction of not only
210 type III IFN but also pro-inflammatory cytokine including IL-6 through the NF-κB
211 signaling pathway. *IL-6* mRNA induction in p-dGdC-transfected NKNT-3/NTCP
212 #28.3.25.13 cells was higher than that in p-dGdC-transfected NKNT-3/NTCP #28.3.8
213 cells (Fig. 5A). In addition, the knockdown of STING reduced *IL-6* mRNA induction in
214 p-dGdC-transfected NKNT-3/NTCP #28.3.25.13 cells (Fig. 5B). Since the
215 phosphorylation of NF-κB p65 at Ser536 was required for the activation of
216 noncanonical NF-κB signaling pathway [17], we next compared the phosphorylation of
217 NF-κB p65 at Ser536 between p-dGdC-transfected NKNT-3/NTCP #28.3.8 cells and
218 #28.3.25.13 cells. Our results indicated that NF-κB p65 was phosphorylated at Ser536
219 in p-dGdC-treated NKNT-3/NTCP #28.3.25.13 cells, but not #28.3.8 cells (Fig. 5C).
220 These results suggest that high-level expression of STING enhances p-dGdC-triggered
221 *IL-6* mRNA induction through the noncanonical NF-κB signaling pathway in
222 NKNT-3/NTCP #28.3.25.13 cells. We next examined whether HBV infection also
223 triggered *IL-6* mRNA induction through the noncanonical NF-κB signaling pathway in
224 NKNT-3/NTCP #28.3.25.13 cells. Interestingly, HBV infection, but not mock or

225 UV-HBV infection, triggered the phosphorylation of NF-κB p65 at Ser536 (Fig. 5D)
226 and subsequently induced *IL-6* mRNA (Fig. 5E) in NKNT-3/NTCP #28.3.25.13 cells.
227 These results suggest that high-level expression of STING is implicated in
228 HBV-triggered pro-inflammatory cytokine induction through the noncanonical NF-κB
229 signaling pathway in NKNT-3/NTCP #28.3.25.13 cells. NKNT-3/NTCP #28.3.25.13
230 cells are a useful tool for studying hepatic carcinogenesis caused by the HBV-triggered
231 inflammatory response through the NF-κB signaling pathway.
232
233 **Discussion**
234 Cytoplasmic DNA or RNA sensors trigger the innate immune responses and the
235 inflammatory responses by recognizing viral PAMPs. We previously reported that one
236 of the cytoplasmic DNA sensors, cGAS, recognized HBV DNA as viral PAMPs and
237 subsequently induced the innate immune response through its adaptor protein, STING
238 [10]. In the present study, we found that the immortalized human hepatocyte NKNT-3
239 cells exhibited HBV susceptibility by stably expressing the exogenous NTCP (Figs. 1C
240 and 1D). Cells of one of the NKNT-3/NTCP cell-derived clones, NKNT-3/NTCP

#28.3.25.13, highly expressed STING and exhibited resistance to HBV through STING-mediated type III IFN induction (Figs. 4C, 4E, and 4F). Interestingly, STING was highly phosphorylated in p–dGdC-transfected NKNT-3/NTCP #28.3.25.13 cells, but not in the parent, #28, #28.3, or #28.3.8 cells (Fig. 4D). However, it is uncertain why the expression and phosphorylation levels of STING differed among the NKNT-3/NTCP cell-derived cell clones. In humans, several single nucleotide polymorphisms (SNP) of STING have been discovered [18]. SNPs of STING have been shown to cause autoinflammatory diseases such as STING-associated vasculopathy with onset in infancy [19] and familial chilblain lupus [20]. These SNPs are implicated in the dysregulation of host innate immune responses and inflammatory responses through a loss-of-function mutation or a gain-of-function mutation of STING. Further analysis is needed to identify the gain-of-function mutation(s) in STING in NKNT-3/NTCP #28.3.25.13 cells.

In the present study, we showed that HBV infection induced type III IFN, but not IFN-β (type I IFN), through a STING-mediating signaling pathway in NKNT-3/NTCP #28.3.25.13 cells (Fig. 5F). Sato et al. previously reported that a cytoplasmic RNA

257 sensor, RIG-I, recognized HBV pgRNA and subsequently induced type III but not type I
258 IFN through its adaptor protein, IPS-1, in human primary hepatocytes [21]. These
259 results suggest that HBV suppresses the induction of type I IFN but not type III IFN.
260 One of the HBV proteins, HBV polymerase, suppressed STING-mediated IFN-β
261 induction by disrupting K63-linked ubiquitination of STING [22]. Another study also
262 reported that HBx bound IPS-1 and suppressed the activation of IFN-β [23]. However,
263 in these studies, it was unclear whether HBV suppressed the induction of type III IFN
264 through these HBV proteins. Our results showed that HBV transiently induced *ISG56*
265 mRNA induction at 5 and 9 days, but not at 13 days, after HBV infection in
266 NKNT-3/NTCP #28.3.25.13 cells (Fig. 3D). This result suggests that HBV possesses
267 two opposite functions to simultaneously trigger or suppress the induction of type III
268 IFN. Further analysis is needed to examine whether or not HBV suppresses the
269 induction of type III IFN.

270 We also showed that HBV infection induced a pro-inflammatory cytokine, IL-6,
271 through the noncanonical NF-κB signaling pathway in NKNT-3/NTCP #28.3.25.13
272 cells (Fig. 5F). STING also mediates host inflammatory responses by triggering its

273 downstream NF-κB signaling pathway [8, 9]. A STING-triggered host inflammatory
274 response has been reported to be associated with hepatic diseases [24, 25]. In
275 nonalcoholic fatty liver disease, STING promotes hepatocyte injury by inducing
276 inflammation [24]. In addition, STING mediates liver injury and fibrosis in mice
277 administered CCl_4 (a chemical inducer of hepatocyte death) [25]. Moreover, based on
278 the results of several previous studies, STING is also thought to play an important role
279 in tumor development [26]. Interestingly, STING may exert two opposite effects
280 (tumor-suppressing and tumor-promoting effects) on tumor development under different
281 situations. For example, in breast cancer, STING and its downstream signaling may
282 suppress the tumor or the cancer metastasis [27, 28]. In contrast, STING is also required
283 for cell survival and regrowth in breast cancer [29, 30]. However, the results of the
284 present study do not clarify whether the HBV-triggered NF-κB signaling pathway
285 causes liver diseases and tumor development. Further analysis will also be needed to
286 examine how HBV causes liver diseases and finally HCC through a STING-mediated
287 NF-κB signaling pathway.

288 In the present study, we established a novel HBV infectious cell culture model by

using NKNT-3 cells. Since NKNT-3 cells exhibit a non-neoplastic phenotype [12], our HBV infectious cell culture model is expected to be a useful tool for the study of hepatic carcinogenesis caused by HBV-triggered innate immune responses and inflammatory responses.

Materials and Methods

Cell culture

Human immortalized hepatocyte NKNT-3 cells, which were kindly provided by N. Kobayashi and M. Namba (Okayama University). Human hepatoma HepG2/NTCP cells were cultured as previously described [10]. HepG2.2.15 Cont, HepG2.2.15 cGAS/STING, and HepG2.2.15 cGAS GSAA/STING cells were maintained in medium including blasticidin and puromycin as previously described [10].

Establishment of an NKNT-3 cell line stably expressing exogenous NTCP and the derivation of its cell clones

NKNT-3 cells stably expressing exogenous NTCP (designated NKNT-3/NTCP cells)

were established as previously described [10]. NKNT-3/NTCP-derived cell clones were isolated from their parental cells by the limited dilution method. We evaluated HBV susceptibility by HBV/NLuc assay [13] and, from the several tens of cell clones obtained, selected a cell clone exhibiting susceptibility or resistance to HBV. By repeating the cell cloning and selection process, we obtained cell clones exhibiting the different levels of susceptibility to HBV.

HBV/NLuc assay

HBV/NLuc was prepared as previously reported [13]. Intracellular NLuc activity was measured at 5, 9, and 13 days after the inoculation of HBV/NLuc. For the measurement of NLuc activity, we used a Nano-Glo luciferase assay system (Promega, Madison, WI, USA). Data are the means ± SD from three independent experiments.

Western blot analysis

Western blot analysis was performed as previously described [31]. Anti-Myc (PL14; Medical & Biological Laboratories, Nagoya, Japan), anti-ISG15 (H-150; Santa Cruz

Biotechnology, Dallas, TX, USA), anti-ISG56, anti-cGAS, anti-phospho-STING (Ser366), anti-STING, anti-phospho-NF-κB p65 (Ser536), anti-NF-κB p65 (Cell Signaling Technology, Beverly, MA, USA), and anti-β-actin (AC-15; Sigma-Aldrich, St. Louis, MO, USA) were used as primary antibodies.

Flow cytometric analysis

Cell surface expression of exogenous NTCP was detected by a flow cytometer as previously reported [32]. Anti-Myc (PL14; Medical & Biological Laboratories), and FITC-conjugated goat anti-mouse antibody (Jackson ImmunoResearch Laboratories, West Grove, PA, USA) were used as primary and secondary antibody, respectively.

Analysis of HBV RNA

HBV was prepared from the supernatant of HepG2.2.15 cells as previously reported [10]. Cells were infected with HBV at 10^3 HBV genome equivalents per cell, unless otherwise described. For the analysis of intracellular HBV RNA after the infection of HBV, we performed quantitative RT-PCR analysis and Northern blot analysis as

previously reported [10].

Quantitative RT-PCR analysis

At 5, 9, and 13 days after HBV inoculation or at 6 hours after the transfection of an *in vitro*-synthesized ligand, p-dGdC (Invivogen, San Diego, CA, USA), we performed quantitative RT-PCR analysis as previously described [33]. For quantitative RT-PCR analysis, we used primer sets previously described for ISG56 [34], IFN-β [34], cGAS [10], STING [10], IL-6 [33], and GAPDH [33]. We also prepared forward and reverse primer sets for IFN-λ1 (5'- CTGGGAAGGGCTGCCACATT-3' (forward) and 5'-TTGAGTGACTCTTCCAAGGCG-3' (reverse)) and IFN-λ2/3 (5'-CAGCTGCAGGTGAGGGAG-3' (forward) and 5'-CTGGGTCAGTGTCAGCGG-3' (reverse)).

RNA interference

The day after mock or HBV infection, we introduced small interfering RNAs (siRNAs) targeting STING or nontargeting siRNAs into NKNT-3/NTCP #28.3.25.13 cells as

353 previously described [35]. At 4 days after the introduction of siRNAs, we isolated the
354 total RNA or cell lysate, and subjected it to quantitative RT-PCR analysis or western
355 blot analysis, respectively.
356
357 **Generation of cells stably expressing exogenous STING**
358 To construct pCX4bleo/HA-STING retroviral vector, we introduced STING (accession
359 no. NM_198282) cDNA containing a full-length ORF into the pCX4bleo/HA retroviral
360 vector as previously reported [36]. pCX4bleo/HA-STING I200N [16] was also
361 constructed using PCR mutagenesis with primers containing base alterations. These
362 vectors were introduced into NKNT-3/NTCP #28.3.8 cells by retroviral transfer and
363 then the cells stably expressing exogenous STING or STING I200N were selected by
364 Zeocin (Thermo Fisher Scientific, Carlsbad, CA, USA).
365
366 **Statistical analysis**
367 Statistical analysis was performed to determine the significance of differences among
368 groups by using Student's *t*-test. $P < 0.05$ was considered statistically significant.

Acknowledgements

We thank Marie Iwado, Masayo Takemoto, and Masato Ono for their technical assistance. We also thank Dr. Tsuyoshi Akagi for the provision of pCX4bleo retroviral vectors. This research was supported by the Japan Agency for Medical Research and Development (AMED) under grant numbers JP17fk0310107 and JP17fk0310103, and by a grant from the Wesco Foundation.

Funding

Japan Agency for Medical Research and Development (AMED)

grant numbers JP17fk0310107 and JP17fk0310103

Wesco Foundation

Author Contributions

HD and NK designed the research. HD performed most of the experiments. HI contributed pCX4bleo HA-STING I200N. NK performed the cell cloning by the limited

dilution method. HD, HI, YU, SS and NK analyzed the data. HD wrote the paper. All authors reviewed the manuscript.

Conflict of interest

The authors declare that they have no conflict of interest.

References

1. Chen DS (1993) From hepatitis to hepatoma: lessons from type B viral hepatitis. *Science* **262:** 369-370

2. Kao JH, Chen DS (2002) Global control of hepatitis B virus infection. *Lancet Infect Dis* **2:** 395-403

3. Sun L, Wu J, Du F, Chen X, Chen ZJ (2013) Cyclic GMP-AMP synthase is a cytosolic DNA sensor that activates the type I interferon pathway. *Science* **339:** 786-791

4. Wu J, Sun L, Chen X, Du F, Shi H, Chen C, Chen ZJ (2013) Cyclic GMP-AMP is an endogenous second messenger in innate immune signaling by cytosolic DNA. *Science* **339:** 826-830

401 5. Ishikawa H, Ma Z, Barber GN (2009) STING regulates intracellular DNA-mediated,
402 type I interferon-dependent innate immunity. *Nature* **461:** 788-792
403 6. Sui H, Zhou M, Imamichi H, Jiao X, Sherman BT, Lane HC, Imamichi T (2017)
404 STING is an essential mediator of the Ku70-mediated production of IFN-λ1 in response
405 to exogenous DNA. *Sci Signal* **10:** eaah5054
406 7. Kotenko SV, Gallagher G, Baurin VV, Lewis-Antes A, Shen M, Shah NK, Langer JA,
407 Sheikh F, Dickensheets H, Donnelly RP (2003) IFN-λs mediate antiviral protection
408 through a distinct class II cytokine receptor complex. *Nat Immunol* **4:** 69-77
409 8. Abe T, Barber GN (2014) Cytosolic-DNA-mediated, STING-dependent
410 proinflammatory gene induction necessitates canonical NF-κB activation through TBK1.
411 *J Virol* **88:** 5328-5341
412 9. Blaauboer SM, Gabrielle VD, Jin L (2014) MPYS/STING-mediated TNF-α, not type
413 I IFN, is essential for the mucosal adjuvant activity of
414 (3'-5')-cyclic-di-guanosine-monophosphate in vivo. *J Immunol* **192:** 492-502
415 10. Dansako H, Ueda Y, Okumura N, Satoh S, Sugiyama M, Mizokami M, Ikeda M, Kato
416 N (2016) The cyclic GMP-AMP synthetase-STING signaling pathway is required for

both the innate immune response against HBV and the suppression of HBV assembly. *FEBS J* **283:** 144-156

11. Yan H, Zhong G, Xu G, He W, Jing Z, Gao Z, Huang Y, Qi Y, Peng B, Wang H, *et al* (2012) Sodium taurocholate cotransporting polypeptide is a functional receptor for human hepatitis B and D virus. *eLife* **1:**, e00049

12. Kobayashi N, Fujiwara T, Westerman KA, Inoue Y, Sakaguchi M, Noguchi H, Miyazaki M, Cai J, Tanaka N, Fox IJ, *et al* (2000) Prevention of acute liver failure in rats with reversibly immortalized human hepatocytes. *Science* **287:** 1258-1262

13. Nishitsuji H, Ujino S, Shimizu Y, Harada K, Zhang J, Sugiyama M, Mizokami M, Shimotohno K (2015) Novel reporter system to monitor early stages of the hepatitis B virus life cycle. *Cancer Sci* **106:** 1616-1624

14. Sells MA, Chen ML, Acs G (1987) Production of hepatitis B virus particles in Hep G2 cells transfected with cloned hepatitis B virus DNA. *Proc Natl Acad Sci USA* **84:** 1005-1009

15. Watashi K, Sluder A, Daito T, Matsunaga S, Ryo A, Nagamori S, Iwamoto M, Nakajima S, Tsukuda S, Borroto-Esoda K, *et al* (2014) Cyclosporin A and its analogs

433 inhibit hepatitis B virus entry into cultured hepatocytes through targeting a membrane
434 transporter, sodium taurocholate cotransporting polypeptide (NTCP). *Hepatology* **59:**
435 1726-1737
436 16. Yin Q, Tian Y, Kabaleeswaran V, Jiang X, Tu D, Eck MJ, Chen ZJ, Wu H (2012)
437 Cyclic di-GMP sensing via the innate immune signaling protein STING. *Mol Cell* **46:**
438 735-745
439 17. Sasaki CY, Barberi TJ, Ghosh P, Longo DL (2005) Phosphorylation of RelA/p65 on
440 Serine 536 Defines an IκBα-independent NF-κB Pathway. *J Biol Chem* **280:**
441 34538-34547
442 18. Li Y, Wilson HL, Kiss-Toth E (2017) Regulating STING in health and disease. *J*
443 *Inflammation* **59:** 14:11
444 19. Liu Y, Jesus AA, Marrero B, Yang D, Ramsey SE, Sanchez GAM, Tenbrock K,
445 Wittkowski H, Jones OY, Kuehn HS, *et al* (2014) Activated STING in a vascular and
446 pulmonary syndrome. *N Engl J Med* **371:** 507-518
447 20. König N, Fiehn C, Wolf C, Schuster M, Cura Costa E, Tüngler V, Alvarez HA,
448 Chara O, Engel K, Goldbach-Mansky R, *et al* (2017) Familial chilblain lupus due to a

449 gain-of-function mutation in STING. *Ann Rheum Dis* **76:** 468-472

450 21. Sato S, Li K, Kameyama T, Hayashi T, Ishida Y, Murakami S, Watanabe T, Iijima S,

451 Sakurai Y, Watashi K, *et al* (2015) The RNA sensor dually functions as an innate sensor

452 and direct antiviral factor for hepatitis B virus. *Immunity* **42:** 123-132

453 22. Liu Y, Li J, Chen J, Li Y, Wang W, Du X, Song W, Zhang W, Lin L, Yuan Z (2015)

454 Hepatitis B virus polymerase disrupts K63-linked ubiquitination of STING to block

455 innate cytosolic DNA-sensing pathways. *J Virol* **89:** 2287-2300

456 23. Kumar M, Jung SY, Hodgson AJ, Madden CR, Qin J, Slagle BL (2011) Hepatitis B

457 virus regulatory HBx protein binds to adaptor protein IPS-1 and inhibits the activation

458 of beta interferon. *J Virol* **85:** 987-995

459 24. Qiao JT, Cui C, Qing L, Wang LS, He TY, Yan F, Liu FQ, Shen YH, Hou XG, Chen

460 L (2018) Activation of the STING-IRF3 pathway promotes hepatocyte inflammation,

461 apoptosis and induces metabolic disorders in nonalcoholic fatty liver disease.

462 *Metabolism* **81:** 13-24

463 25. Iracheta-Vellve A, Petrasek J, Gyongyosi B, Satishchandran A, Lowe P, Kodys K,

464 Catalano D, Calenda CD, Kurt-Jones EA, Fitzgerald KA, *et al* (2016) Endoplasmic

Reticulum Stress-induced Hepatocellular Death Pathways Mediate Liver Injury and Fibrosis via Stimulator of Interferon Genes. *J Biol Chem* **291:** 26794-26805

26. He L, Xiao X, Yang X, Zhang Z, Wu L, Liu Z (2017) STING signaling in tumorigenesis and cancer therapy: A friend or foe? *Cancer Lett* **402:** 203-212

27. Bhatelia K, Singh A, Tomar D, Singh K, Sripada L, Chagtoo M, Prajapati P, Singh R, Godbole MM, Singh R (2014) Antiviral signaling protein MITA acts as a tumor suppressor in breast cancer by regulating NF-kappaB induced cell death. *Biochim Biophys Acta* **1842:** 144-153

28. Chandra D, Quispe-Tintaya W, Jahangir A, Asafu-Adjei D, Ramos I, Sintim HO, Zhou J, Hayakawa Y, Karaolis DK, Gravekamp C (2014) STING ligand c-di-GMP improves cancer vaccination against metastatic breast cancer. *Cancer Immunol Res* **2:** 901-910

29. Lemos H, Mohamed E, Huang L, Ou R, Pacholczyk G, Arbab AS, Munn D, Mellor AL (2016) STING promotes the growth of tumors characterized by low antigenicity via IDO activation. *Cancer Res* **76:** 2076-2081

30. Gaston J, Cheradame L, Yvonnet V, Deas O, Poupon MF, Judde JG, Cairo S, Goffin

481 V (2016) Intracellular STING inactivation sensitizes breast cancer cells to genotoxic
482 agents. *Oncotarget* **7:** 77205-77224

483 31. Dansako H, Ikeda M, Kato N (2007) Limited suppression of the interferon-beta
484 production by hepatitis C virus serine protease in cultured human hepatocytes. *FEBS J*
485 **274:** 4161-4176

486 32. Dansako H, Imai H, Ueda Y, Satoh S, Wakita T, Kato N (2018) ULBP1 is induced
487 by hepatitis C virus infection and is the target of the NK cell-mediated innate immune
488 response in human hepatocytes. *FEBS Open Bio* **8:** 361-371

489 33. Dansako H, Ikeda M, Ariumi Y, Wakita T, Kato N (2009) Double-stranded
490 RNA-induced interferon-beta and inflammatory cytokine production modulated by
491 hepatitis C virus serine proteases derived from patients with hepatic diseases. *Arch Virol*
492 **154:** 801-810

493 34. Dansako H, Yamane D, Welsch C, McGivern DR, Hu F, Kato N, Lemon SM (2013) Class A
494 scavenger receptor 1 (MSR1) restricts hepatitis C virus replication by mediating Toll-like
495 receptor 3 recognition of viral RNAs produced in neighboring cells. *PLoS Pathog* **9:** e1003345

496 35. Dansako H, Hiramoto H, Ikeda M, Wakita T, Kato N (2014) Rab18 is required for viral
497 assembly of hepatitis C virus through trafficking of the core protein to lipid droplets. *Virology*
498 **462-463C:** 166-174

499 36. Dansako H, Naganuma A, Nakamura T, Ikeda F, Nozaki A, Kato N (2003)
500 Differential activation of interferon-inducible genes by hepatitis C virus core protein
501 mediated by the interferon stimulated response element. *Virus Res* **97:** 17-30

502

503 **Figure legends**

504 **Figure 1 - The immortalized human hepatocyte cell line NKNT-3 exhibited**
505 **susceptibility to HBV by expressing exogenous NTCP.**

506 A Western blot analysis of exogenous NTCP in NKNT-3/NTCP cells. Anti-Myc
507 antibody was used for the detection of NTCP-Myc in NKNT-3/NTCP cells. β-actin was
508 included as a loading control.

509 B Flow cytometric analysis of the cell surface NTCP in NKNT-3/Control cells,
510 NKNT-3/NTCP cells, or HepG2/NTCP cells. Signals of the cell surface NTCP are
511 shown in green. An isotype control was used as a negative control (violet area).

C Comparison of NLuc activity after HBV/NL inoculation between NKNT-3/Control cells and NKNT-3/NTCP cells. Intracellular NLuc activity was measured at 5, 9, and 13 days after HBV/NL inoculation. $^{**}P < 0.01$, $^{***}P < 0.001$ versus HBV/NL-infected NKNT-3/Cont cells.

D Quantitative RT-PCR analysis of the amount of HBV total transcript in HBV-infected NKNT-3/Control cell or NKNT-3/NTCP cells. The supernatant of HepG2.2.15 cells was used as an HBV inoculum. The amounts of HBV total transcript were measured at 5, 9, and 13 days after HBV inoculation. $^{**}P < 0.01$, $^{***}P < 0.001$ versus HBV-infected NKNT-3/Cont cells.

E, F Comparison of the susceptibility to HBV between HepG2/NTCP cells and NKNT-3/NTCP cells. Intracellular NLuc activity was measured after HBV/NL inoculation. The amounts of HBV total transcript and the pgRNA were measured after HBV inoculation by quantitative RT-PCR analysis. $^{**}P < 0.01$, $^{***}P < 0.001$ versus HBV/NL- or HBV-infected HepG2/NTCP cells, respectively.

G Functional analysis of NTCP in NKNT-3/NTCP cells using CsA as an HBV-entry inhibitor. CsA was administered before and during HBV inoculation. $^{*}P < 0.05$, $^{***}P <$

528 0.001 versus 0 μM of CsA-administered HBV-infected cells.

529

530 **Figure 2 - The level of susceptibility to HBV in NKNT-3/NTCP #28.3.8 cells**

531 **approximated that in HepG2/NTCP cells.**

532 A Outline of cell cloning by the limited dilution method. NKNT-3/NTCP #28.3.8

533 cells were selected by three-round limited dilution. Red arrows with solid lines show the

534 selection of a cell clone exhibiting higher susceptibility to HBV.

535 B Comparison of susceptibility to HBV among parent NKNT-3/NTCP cells and their

536 derived cell clones by using HBV/NL assay. $^{**}P < 0.01$, $^{***}P < 0.001$ versus

537 HBV/NL-infected parent NKNT-3/NTCP cells.

538 C Flow cytometric analysis of the cell surface NTCP in their derived cell clones.

539 Signals of the cell surface NTCP are shown in green. An isotype control was used as a

540 negative control (violet area).

541 D Comparison of the amounts of HBV total transcript after HBV infection among

542 parent NKNT-3/NTCP cells and their derived cell clones. The amount of HBV total

543 transcript was measured after HBV infection by quantitative RT-PCR analysis. $^{*}P <$

544 0.05 versus HBV-infected parent NKNT-3/NTCP cells.

545 E, F Comparison of susceptibility to HBV between HepG2/NTCP cells and
546 NKNT-3/NTCP #28.3.8 cells. Intracellular NLuc activity or the amounts of HBV total
547 transcript were measured as described in Figs. 1E and 1F. NS; not significant, **P <
548 0.01, ***P < 0.001 versus HBV/NL- or HBV-infected HepG2/NTCP cells, respectively.

549 G Comparison of susceptibility to HBV between HepG2/NTCP cells and
550 NKNT-3/NTCP #28.3.8 cells by Northern blot analysis. Total RNA was isolated from
551 HBV-infected cells at 13 days after HBV inoculation. 28S rRNA and 18S rRNA were
552 included as a loading control. NKNT-3/NTCP #28.8.4 is another clone, which has been
553 estimated to exhibit susceptibility to HBV by HBV/NL assay (data not shown).

554

555 **Figure 3 – HBV induced type III IFN in NKNT-3/NTCP #28.3.25.13 cells exhibiting**
556 **resistance to HBV.**

557 A Outline of cell cloning by the limited dilution method. NKNT-3/NTCP
558 #28.3.25.13 and #28.3.30.20.3 cells were selected by their distinct serial limited dilution,
559 respectively. Blue arrows with dashed lines show the selection of a cell clone exhibiting

resistance to HBV.

B Quantitative RT-PCR analysis of the amounts of HBV total transcript in HBV-infected NKNT-3/NTCP #28.3.8, #28.3.25.13, or #28.3.30.20.3 cells. *$P < 0.05$, **$P < 0.01$ versus HBV-infected NKNT-3N #28.3.8 cells.

C Western blot analysis of ISG56 in HBV-infected NKNT-3/NTCP #28.3.8, #28.3.25.13, or #28.3.30.20.3 cells. Cell lysates were prepared from mock- or HBV-infected cells at 5 days after HBV inoculation.

D Quantitative RT-PCR analysis of *ISG56* mRNA in HBV-infected NKNT-3/NTCP #28.3.8 or #28.3.25.13 cells. Cells were infected with HBV at 10^3 or 10^4 HBV genome equivalents per cell, respectively. Each mRNA level was calculated relative to the level in mock-infected NKNT-3/NTCP #28.3.25.13 cells, which was set at 1. *$P < 0.05$, **$P < 0.01$, ***$P < 0.001$ versus mock-infected NKNT-3N #28.3.25.13 cells.

E Quantitative RT-PCR analysis of *IFN-λ1* and *IFN-λ2/3* mRNA in HBV-infected NKNT-3/NTCP #28.3.8 or #28.3.25.13 cells. Cells were infected with HBV at 10^3 or 10^4 HBV genome equivalents per cell, respectively. Each mRNA level was calculated as described in Fig. 3D. ND, not detected. NS; not significant, *$P < 0.05$, **$P < 0.01$

versus mock-infected NKNT-3/NTCP #28.3.25.13 cells.

F Quantitative RT-PCR analysis of *IFN-β* mRNA in HBV-infected NKNT-3/NTCP #28.3.8 or #28.3.25.13 cells. Cells were infected with HBV at 10^3 or 10^4 HBV genome equivalents per cell, respectively. Each mRNA level was calculated as described in Fig. 3D. NS; not significant versus mock-infected NKNT-3/NTCP #28.3.25.13 cells.

G (left panel) Quantitative RT-PCR analysis of the amounts of HBV total transcript in mock-, HBV-, or UV-HBV-infected NKNT-3/NTCP #28.3.25.13 cells. (right panels) Quantitative RT-PCR analysis of *IFN-λ1* mRNA in mock-, HBV-, or UV-HBV-infected NKNT-3/NTCP #28.3.25.13 cells. Each mRNA level was calculated as described in Fig. 3D. $^{**}P < 0.01$ versus mock- or UV-HBV-infected NKNT-3/NTCP #28.3.25.13 cells, respectively.

H Western blot analysis of ISG15 and ISG56 in mock-, HBV-, or UV-HBV-infected NKNT-3/NTCP #28.3.25.13 cells. The cell lysate was prepared as described in Fig. 3C.

I Quantitative RT-PCR analysis of *IFN-λ1*, *IFN-λ2/3*, and *IFN-β* mRNA in HepG2.2.15 cGAS/STING cells. Each mRNA level was calculated relative to the level in HepG2.2.15 Cont cells, which was set at 1. $^{*}P < 0.05$, $^{**}P < 0.01$ versus HepG2.2.15

592 Cont cells or HepG2.2.15 cGAS GSAA/STING cells, respectively.

593

594 **Figure 4 – High-level expression of STING was implicated in HBV-triggered type**

595 **III IFN induction in NKNT-3/NTCP #28.3.25.13 cells.**

596 A (upper panel) Quantitative RT-PCR analysis of *ISG56* and *IFN-λ1* mRNA in

597 p-dGdC-transefected NKNT-3/NTCP #28.3.8 or #28.3.25.13 cells. Each mRNA level

598 was calculated relative to the level in vehicle-transfected NKNT-3/NTCP #28.3.25.13

599 cells, which was set at 1. ***$P < 0.001$ versus p-dGdC-transfected NKNT-3/NTCP

600 #28.3.8 cells. (lower panel) Western blot analysis of ISG56 in p-dGdC-transefected

601 NKNT-3/NTCP #28.3.8 or #28.3.25.13 cells. The cell lysate was prepared as described

602 in Fig. 3C.

603 B Quantitative RT-PCR analysis of *cGAS* and *STING* mRNA in NKNT-3/NTCP

604 #28.3.8 or #28.3.25.13 cells. Each mRNA level was calculated relative to the level in

605 NKNT-3/NTCP #28.3.25.13 cells, which was set at 1. NS; not significant, ***$P < 0.001$

606 versus NKNT-3/NTCP #28.3.8 cells.

607 C Western blot analysis of cGAS and STING in NKNT-3/NTCP #28.3.8 or

#28.3.25.13 cells.

D (upper-left panel) Quantitative RT-PCR analysis of *IFN-λ1* mRNA in the parent NKNT-3/NTCP cells and in the several cell clones derived from them after transfection with p-dGdC. Each mRNA level was calculated relative to the level in NKNT-3/NTCP #28.3.25.13 cells transfected with vehicle, which was set at 1. NS; not significant, ***P* < 0.01 versus p-dGdC-transfected parent NKNT-3/NTCP cells. (lower-left panel) Western blot analysis of phosphorylated STING at Ser366 in the original NKNT-3/NTCP cells and in the several cell clones derived from them after transfection with p-dGdC. The cell lysate was prepared as described in Fig. 3C. (upper-right panel) Quantitative RT-PCR analysis of *IFN-λ1* mRNA in NKNT-3/NTCP #28.3.25.13 cells transfected with STING-specific (designated NKNT-3/NTCP #28.3.25.13 siSTING) or control (designated NKNT-3/NTCP #28.3.25.13 siCont) siRNA followed by p-dGdC. Each mRNA level was calculated relative to the level in vehicle-transfected NKNT-3/NTCP #28.3.25.13 siCont cells, which was set at 1. ****P* < 0.001 versus p-dGdC-transfected NKNT-3/NTCP #28.3.25.13 siCont cells. (lower-right panel) Western blot analysis of phosphorylated STING at Ser366 in NKNT-3/NTCP

624 #28.3.25.13 siSTING cells after transfection with p-dGdC. The cell lysate was prepared
625 as described in Fig. 3C.
626 E (upper panel) Quantitative RT-PCR analysis of *IFN-λ1* mRNA in mock- or
627 HBV-infected NKNT-3/NTCP #28.3.25.13 siSTING cells or NKNT-3/NTCP
628 #28.3.25.13 siCont cells. Each mRNA level was calculated relative to the level in
629 mock-infected NKNT-3/NTCP #28.3.25.13 siCont cells, which was set at 1. (lower
630 panel) Western blot analysis of ISG56 in HBV-infected NKNT-3/NTCP #28.3.25.13
631 siCont cells or NKNT-3/NTCP #28.3.25.13 siSTING cells. The cell lysate was prepared
632 as described in Fig. 3C. $^{**}P < 0.01$ versus HBV-infected NKNT-3/NTCP #28.3.25.13
633 siCont cells.
634 F Quantitative RT-PCR analysis of the amount of HBV total transcript in
635 HBV-infected NKNT-3/NTCP #28.3.25.13 siCont cells or NKNT-3/NTCP #28.3.25.13
636 siSTING cells. $^{**}P < 0.01$ versus HBV-infected NKNT-3/NTCP #28.3.25.13 siCont
637 cells.
638 G (upper panel) Quantitative RT-PCR analysis of *IFN-λ1* mRNA in mock- or
639 HBV-infected NKNT-3/NTCP #28.3.8 cells stably expressing exogenous STING wild

type (designated NKNT-3/NTCP #28.3.8 STING wt) or STING I200N (designated NKNT-3/NTCP #28.3.8 STING I200N). Each mRNA level was calculated relative to the level in HBV-infected NKNT-3/NTCP #28.3.8 STING I200N cells, which was set at 1. ND, not detected. ***$P < 0.001$ versus HBV-infected NKNT-3/NTCP #28.3.8 STING I200N cells. (lower panel) Western blot analysis of ISG56 in HBV-infected NKNT-3/NTCP #28.3.8 STING wt cells or NKNT-3/NTCP #28.3.8 STING I200N cells. The cell lysate was prepared as described in Fig. 3C.

H Quantitative RT-PCR analysis of the amount of HBV total transcript in HBV-infected NKNT-3/NTCP #28.3.8 STING wt cells or NKNT-3/NTCP #28.3.8 STING I200N cells. ***$P < 0.001$ versus HBV-infected NKNT-3/NTCP #28.3.8 STING I200N cells.

Figure 5 – High-level expression of STING was required for HBV-triggered inflammatory response in NKNT-3/NTCP #28.3.25.13 cells.

A (upper panel) Quantitative RT-PCR analysis of *IL-6* mRNA in p-dGdC-transfected NKNT-3/NTCP #28.3.8 or #28.3.25.13 cells. Each mRNA level was calculated relative

to the level in vehicle-transfected NKNT-3/NTCP #28.3.25.13 cells, which was set at 1. $^{**}P < 0.01$ versus p-dGdC-transfected NKNT-3/NTCP #28.3.8 cells. (lower panel) Western blot analysis of IL-6 in p-dGdC-transfected NKNT-3/NTCP #28.3.8 or #28.3.25.13 cells. The cell lysate was prepared as described in Fig. 3C.

B (upper panel) Quantitative RT-PCR analysis of *IL-6* mRNA in p-dGdC-transfected NKNT-3/NTCP #28.3.25.13 siCont cells or NKNT-3/NTCP #28.3.25.13 siSTING cells. Each mRNA level was calculated relative to the level in vehicle-transfected NKNT-3/NTCP #28.3.25.13 siCont cells, which was set at 1. $^{**}P < 0.01$ versus p-dGdC-transfected NKNT-3/NTCP #28.3.25.13 siCont cells. (lower panel) Western blot analysis of IL-6 in p-dGdC-transfected NKNT-3/NTCP #28.3.25.13 siCont cells or NKNT-3/NTCP #28.3.25.13 siSTING cells. The cell lysate was prepared as described in Fig. 3C.

C Western blot analysis of phosphorylated NF-κB p65 at Ser536 in p-dGdC-transfected NKNT-3/NTCP #28.3.8 or #28.3.25.13 cells.

D Western blot analysis of phosphorylated NF-κB p65 at Ser536 in mock-, HBV-, or UV-HBV-infected NKNT-3/NTCP #28.3.25.13 cells.

672 E (upper panel) Quantitative RT-PCR analysis of *IL-6* mRNA in mock-, HBV-, or
673 UV-HBV-infected NKNT-3/NTCP #28.3.25.13 cells. Each mRNA level was calculated
674 as described in Fig. 3D. ***$P < 0.001$ versus mock- or UV-HBV-infected
675 NKNT-3/NTCP #28.3.25.13 cells, respectively. (lower panel) Western blot analysis of
676 *IL-6* mRNA in mock-, HBV-, or UV-HBV-infected NKNT-3/NTCP #28.3.25.13 cells.
677 F Proposed model of the HBV-triggered host innate immune response and
678 inflammatory response through STING.

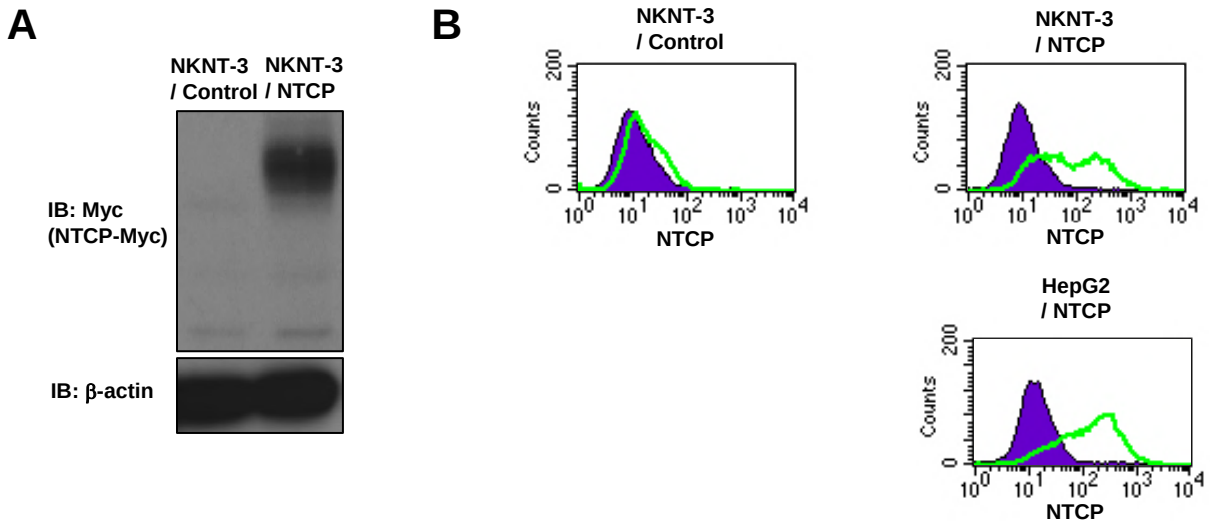

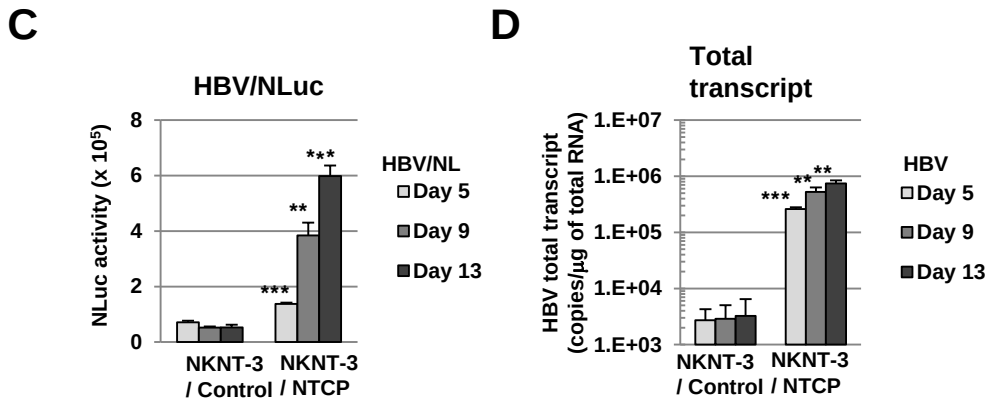

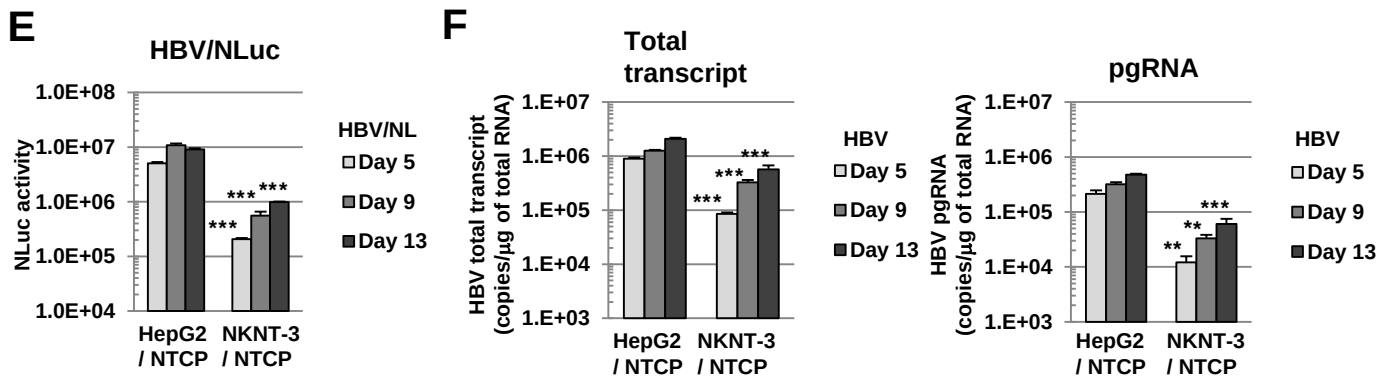

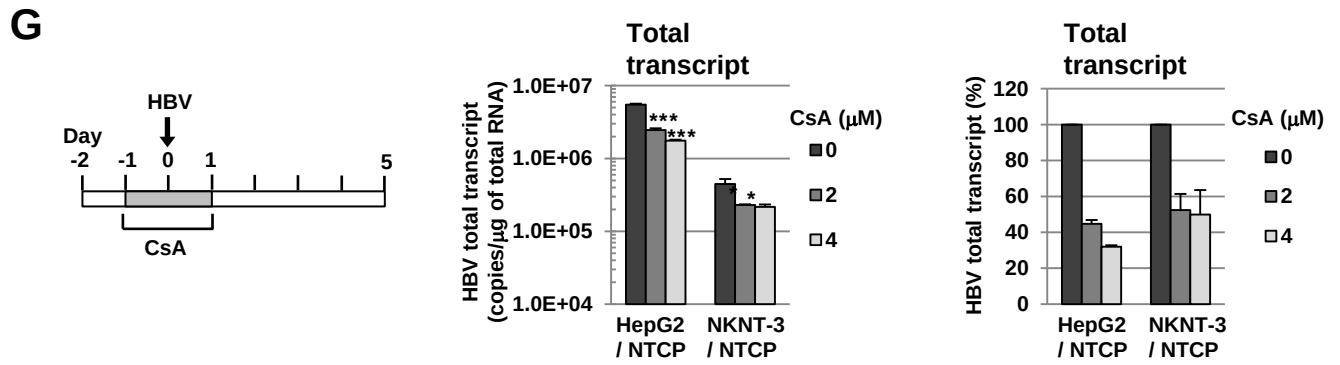

Dansako et al.
Figs. 1

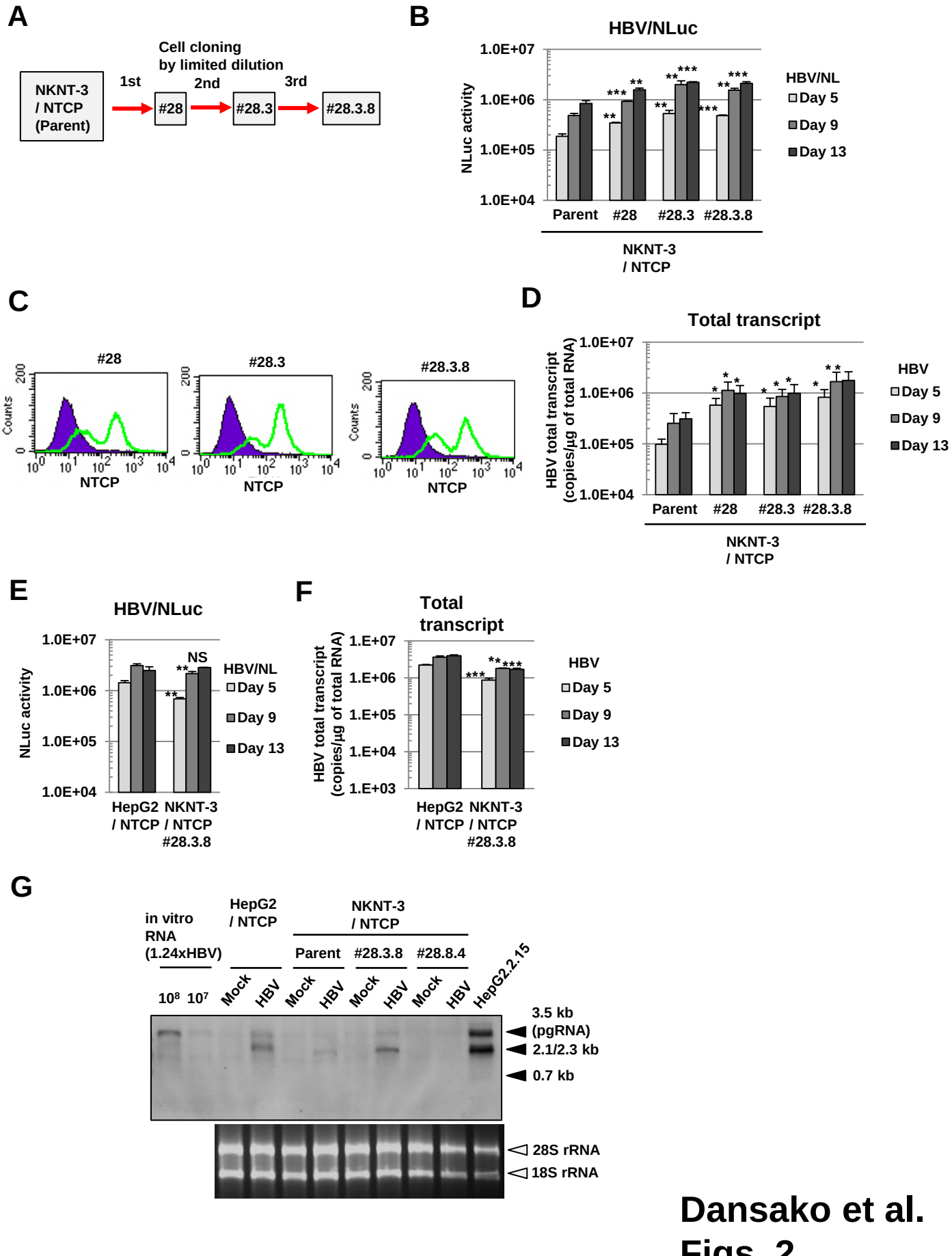

Dansako et al.
Figs. 2

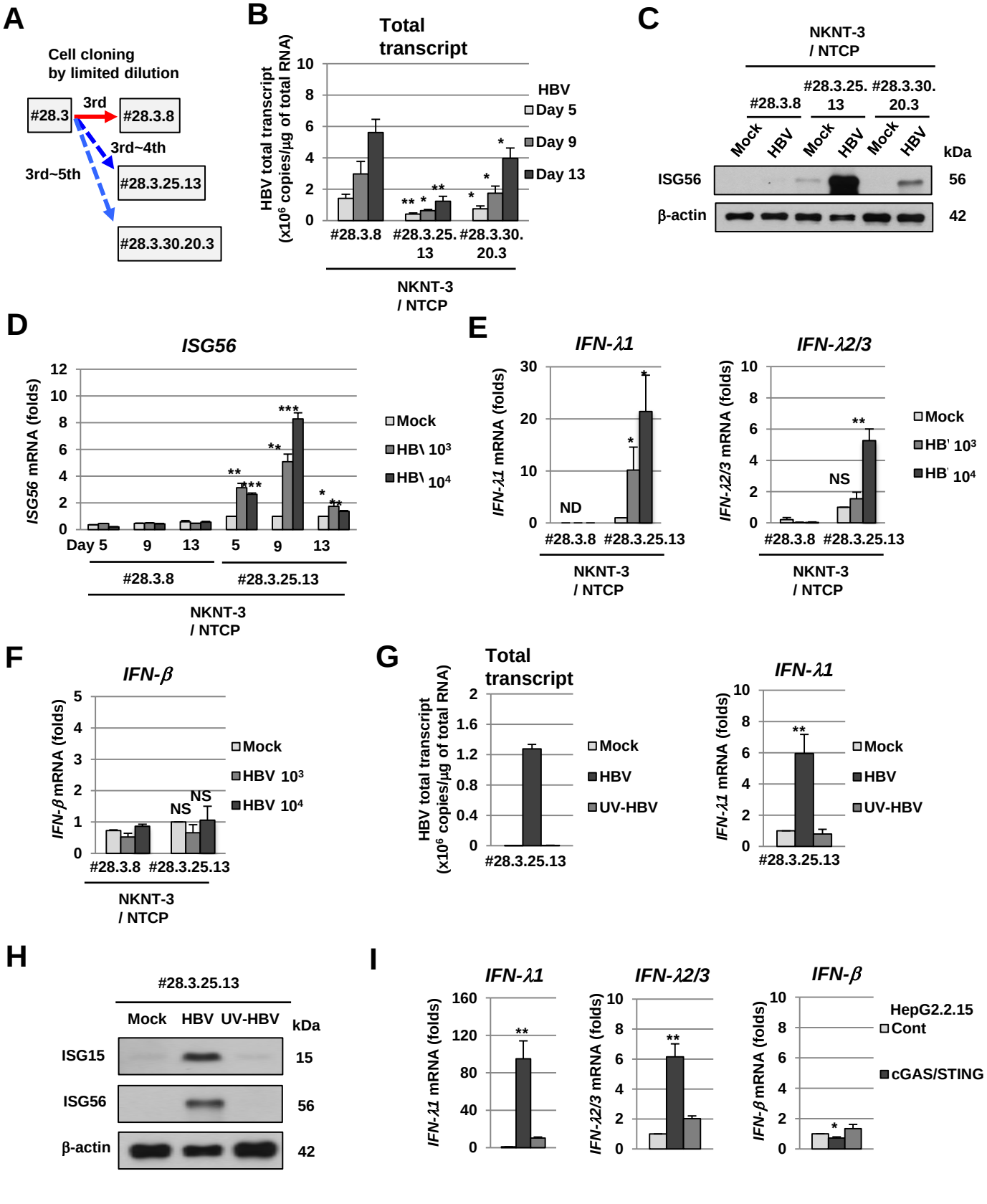

Dansako et al.
Figs. 3

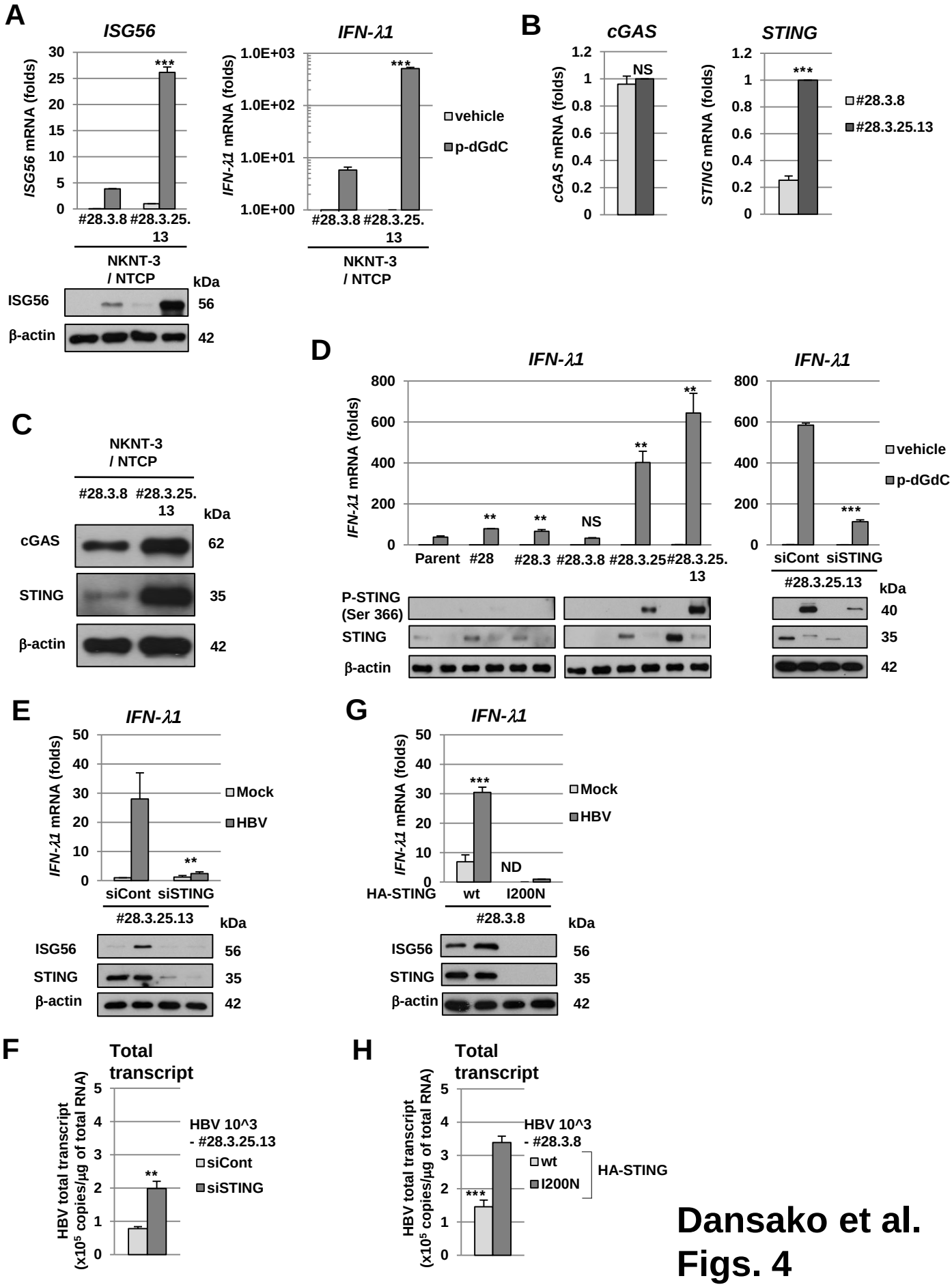
A
ISG56
ISG56 mRNA (folds)
30
25
20
15
10
5
0
***
#28.3.8
#28.3.25.13
NKNT-3 / NTCP
IFN-λ1
IFN-λ1 mRNA (folds)
1.0E+03
1.0E+02
1.0E+01
1.0E+00
***
vehicle
p-dGdC
kDa
ISG56
56
β-actin
42
B
cGAS
cGAS mRNA (folds)
1.2
1
0.8
0.6
0.4
0.2
0
NS
STING
STING mRNA (folds)
***
#28.3.8
#28.3.25.13
C
NKNT-3 / NTCP
#28.3.8
#28.3.25.13
kDa
cGAS
62
STING
35
β-actin
42
D
IFN-λ1
IFN-λ1 mRNA (folds)
800
600
400
200
0
**
**
NS
**
**
Parent
#28
#28.3
#28.3.8
#28.3.25
#28.3.25.13
P-STING (Ser 366)
STING
β-actin
IFN-λ1
siCont
siSTING
***
vehicle
p-dGdC
#28.3.25.13
kDa
40
35
42
E
IFN-λ1
IFN-λ1 mRNA (folds)
50
40
30
20
10
0
Mock
HBV
**
siCont
siSTING
#28.3.25.13
kDa
ISG56
56
STING
35
β-actin
42
G
IFN-λ1
IFN-λ1 mRNA (folds)
50
40
30
20
10
0
***
Mock
HBV
ND
HA-STING
wt
I200N
#28.3.8
kDa
ISG56
56
STING
35
β-actin
42
F
Total transcript
HBV total transcript (x10⁵ copies/μg of total RNA)
5
4
3
2
1
0
**
HBV 10^3 - #28.3.25.13
siCont
siSTING
H
Total transcript
HBV total transcript (x10⁵ copies/μg of total RNA)
5
4
3
2
1
0
***
HBV 10^3 - #28.3.8
wt
I200N
HA-STING
Dansako et al.
Figs. 4

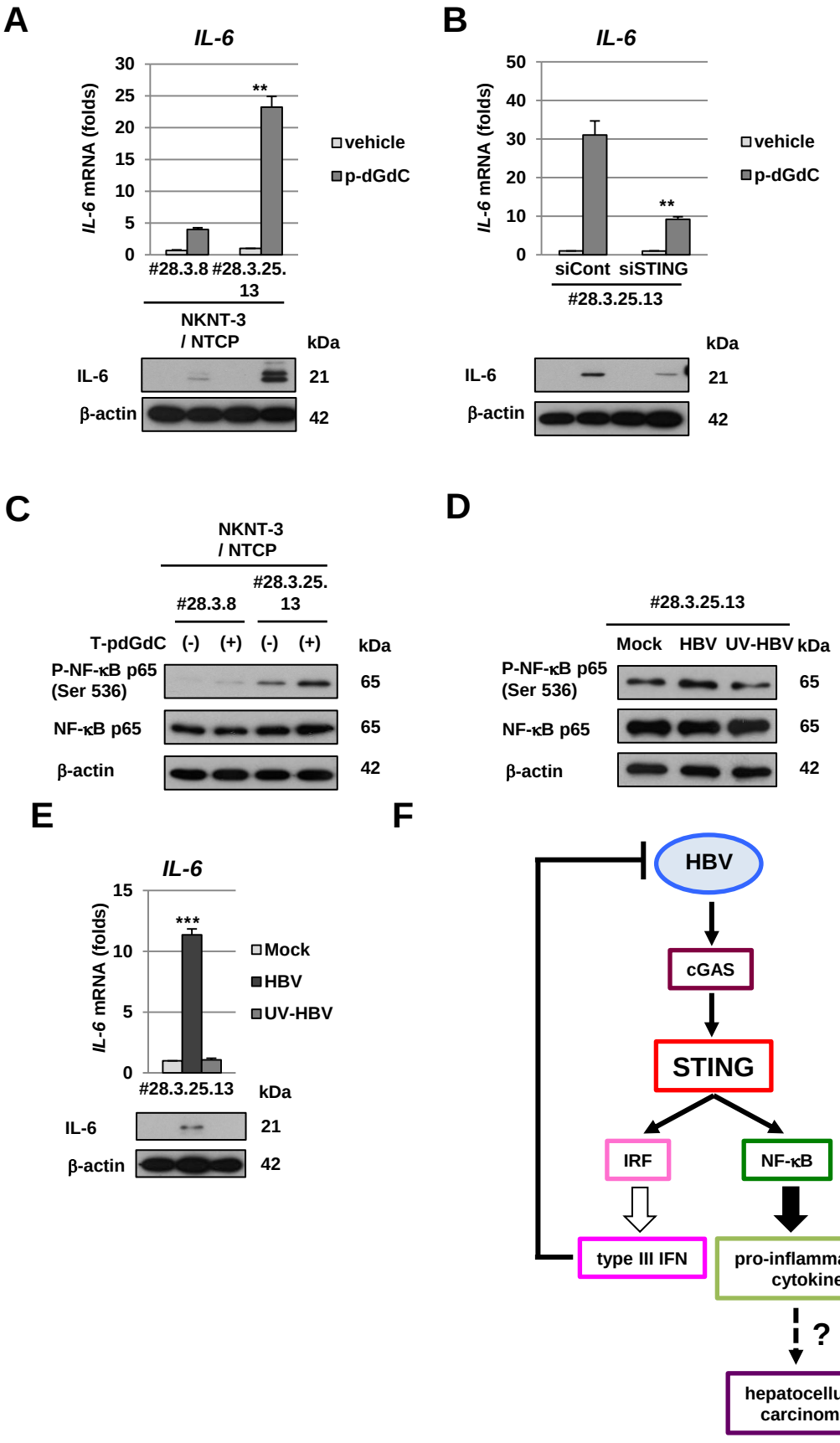

Dansako et al.
Figs. 5